EXPERIMENTAL AND NUMERICAL STUDY ON THE MATERIAL-DEPENDENT VIBRATIONAL RESPONSE OF 3D-PRINTED ANKLE-FOOT ORTHOSES (AFOs)

STUDIU EXPERIMENTAL ȘI NUMERIC ASUPRA RĂSPUNSULUI VIBRAȚIONAL DEPENDENT DE MATERIAL AL ORTEZELOR GLEZNĂ-PICIOR (AFOs) IMPRIMATE 3D

URSACHE Robert-Ionuț[1], PAVEL Cristian[2], MUCENICA Ștefan-Leonard[3], DEACONU Marius[4]

[1,2]Technical University of Civil Engineering, Bucharest, Romania - robionut@gmail.com
[3]Enfebiome (bioengineering initiative), Bucharest, Romania – stefanmucenica@enfebiome.ch
[4]INCDT COMOTI – Acoustic and Vibration – marius.deaconu@comoti.ro

Rezumat: Această cercetare combină testarea in vitro și simulările in silico pentru a identifica și compara comportamentul modal al ortezelor gleznă-picior (AFO) imprimate 3D, fabricate din doi polimeri comuni: acid polilactic (PLA) și polietilen tereftalat glicol (PETG).
Ortezele au fost testate în două condiții dinamice: excitație tranzitorie indusă de teste cu ciocan de impact și excitații armonice generate de un agitator electrodinamic.
Analizele cu elemente finite corespunzătoare au fost efectuate în FEBio (activare cu spectru larg în răspunsul tranzitoriu cu un impuls) și PrePoMax (analiză modală). Semnalele de răspuns experimentale și simulate au fost analizate în domeniul frecvenței pentru a identifica principalele frecvențe de rezonanță, care au fost apoi comparate între toate metodele.
Testele virtuale și de laborator au arătat răspunsuri modale comparabile, frecvențele naturale prezise numeric rămânând în limita a ±2 Hz față de valorile experimentale. Datorită rigidității sale mai mari, PLA a prezentat frecvențe naturale cu aproximativ 10-20 Hz mai mari decât primul până la al treilea mod de vibrație identificat pentru orteza PETG în testarea experimentală.
Aceste descoperiri confirmă fezabilitatea utilizării unor soluții open-source pentru studierea și proiectarea sistemelor ortetice sensibile la vibrații, în special atunci când accesul la echipamente experimentale avansate este limitat.
Cuvinte cheie: orteză gleznă-picior (AFO) imprimată 3D; PLA; PETG; analiza vibrațiilor; analiza modală; simulare open-source; FEBio; PrePoMax; modelare cu elemente finite (FEM); validare experimentală.

Abstract: This research combines in-vitro testing and in-silico simulations to identify and compare the modal behavior of 3D-printed ankle–foot orthoses (AFOs) fabricated from two common polymers: polylactic acid (PLA) and polyethylene terephthalate glycol (PETG).
The orthoses were tested under two dynamic conditions: transient excitation induced by impact hammer tests, and harmonic excitations generated by an electrodynamic shaker.
Corresponding finite element analyses were performed in FEBio (large spectrum activation in the transient response with an impulse) and PrePoMax (modal analysis). The experimental and simulated response signals were analyzed in the frequency domain to identify the main resonance frequencies, which were then compared across all methods.
Virtual and laboratory testing showed comparable modal responses, with the numerically predicted natural frequencies remaining within ±2 Hz of the experimental values. Due to its higher stiffness, PLA exhibited natural frequencies approximately 10–20 Hz higher than the first to third vibration modes identified for the PETG orthosis in the experimental testing.
These findings confirm the feasibility of using open-source solvers for studying and designing vibration-sensitive orthotic systems, particularly when access to advanced experimental equipment is limited.

Keywords: 3D-printed ankle-foot orthosis (AFO); PLA; PETG; vibration analysis; modal analysis; open-source simulation; FEBio; PrePoMax; finite element modeling (FEM); experimental validation.

1. INTRODUCTION

Orthotic devices are widely used in biomechanical rehabilitation to support, stabilize, or correct functional impairments of the musculoskeletal system [1]. Their integration into modern therapeutic approaches has been increasingly supported by advances in design, materials, and digital fabrication techniques such as additive manufacturing (specifically 3d printing) [2]. Recent interest has also grown around the controlled application of mechanical vibrations in orthoses, with the potential to enhance neuromuscular activation, improve proprioception, and accelerate recovery processes [3].

Despite these developments, the dynamic behavior of orthoses under vibratory excitation remains poorly understood. Most studies focus on static load-bearing performance, while the influence of frequency, resonance, and material damping is often overlooked [4]. Moreover, few investigations compare experimental measurements with numerical models, especially using open-source platforms accessible for research and clinical prototyping [5].

This study addresses these limitations by combining physical vibration testing with finite element simulations using open-source software environments. Two common 3D-printing materials – PLA and PETG – were used to fabricate ankle–foot orthoses (AFOs), which were then tested under **transient (impulsive)** and **steady-state (harmonic)** excitation conditions. The objective is to evaluate the vibration response, identify modal characteristics, and compare results between simulation and experiment. The findings aim to promote the integration of validated open-source simulation tools into the early design stages of vibration-sensitive orthotic systems.

From a theoretical standpoint, the vibration behavior of an orthotic structure can be described by the general vector equation of motion for a multi-degree-of-freedom system:

$$\boldsymbol{M\ddot{u} + C\dot{u} + Ku = f}(t) \qquad (1)$$

where $\boldsymbol{M}$, $\boldsymbol{C}$, and $\boldsymbol{K}$ represent the mass, damping, and stiffness matrices; u is the displacement vector, while its first and second time derivatives correspond to velocity and acceleration. The external excitation **f**(t) is balanced by the inertia, damping, and stiffness forces represented by these matrices, applied to the respective motion vectors.

It is important to note that bold symbols denote matrices and vectors, while scalars are written in plain text. The displacement vector and its derivatives depend on several variables, such as time (t), initial conditions, and the external excitation (**f**(t)).

In the case of a **free (natural) response**, no external forces act on the system ($f(t) = 0$), and the motion depends on the structural properties alone:

$$\boldsymbol{M\ddot{u} + C\dot{u} + Ku} = 0 \qquad (2)$$

For **forced vibrations**, the external excitation can be expressed as a sinusoidal input:

$$\boldsymbol{f}(t) = \boldsymbol{f_0} sin(2\pi ft + \varphi) = \boldsymbol{f_0} sin\,(\omega t + \varphi), \qquad (3)$$

where $\boldsymbol{f_0}$ is the amplitude vector, f is the frequency, $\omega = 2\pi f$ is the angular frequency and φ is the phase of the excitation vector $\boldsymbol{f}(t)$.

In practical applications, the external input can also be represented as a finite approximation of the Dirac delta impulse (triangular signal), expressed in its generic vectorial form as follows:

$$\delta(t) = \begin{cases} 2\boldsymbol{\Delta_0} t, [0, T/2] \\ -2\boldsymbol{\Delta_0}\left(\frac{1}{T} - 1\right)[T/2\,, T] \\ 0, elsewere \end{cases} \quad (4)$$

where $\boldsymbol{\Delta}_0$ is the peak of the finite impulse $\delta(t)$, while T is its period.

Experimentally, the forced response was investigated using a shaker and an impact excitation (hammer test). In numerical simulations, the same physical principles were reproduced: transient (impulse-based) analysis in FEBio and free-vibration modal analysis in PrePoMax.

2. MATERIALS AND METHODS

2.1 Materials and 3D printing

Two commonly used thermoplastics for 3D printing were selected for this study: polylactic acid (PLA) and polyethylene terephthalate glycol-modified (PETG). Both filaments were supplied by AzureFilm (Slovenia) and were chosen for their availability, ease of processing, and mechanical properties relevant to orthotic applications [7][8].

Custom ankle–foot orthoses (AFOs) were designed using CAD software based on standard anatomical dimensions and subsequently scaled down proportionally to fit the 3D printer's build volume (Fig. 1).

Figure 1. Bounding volume of the orthosis represented as a box of 82.6 × 92.0 × 55.5 mm³

The reduced size preserved the geometric proportions and stiffness distribution of the full-scale design, allowing efficient fabrication while maintaining structural characteristics relevant for vibration testing.

The models were fabricated using a desktop FDM 3D printer equipped with a 0.4 mm nozzle and a 0.2 mm layer height. Both materials were printed with 100% infill to ensure structural integrity and consistency between samples. Printing speed was set to 50 mm/s. The nozzle temperature was 210°C for PLA and 240°C for PETG, with the heated bed maintained at 60°C for both. Support structures and a brim adhesion layer were used to ensure dimensional accuracy and prevent detachment during printing. No post-processing or annealing was performed after fabrication.

The mechanical properties of PLA and PETG used in this study were determined based on experimental tensile tests and literature data [7][8], complemented by a brief sensitivity analysis performed within the natural response simulations. Isotropic linear elastic properties were assigned

to both materials, under small deformation conditions (Tab. 1). Density was estimated from the measured mass and volume of the orthoses. Since no significant differences were found, the same density value was assigned to both PETG and PLA devices.

Table 1. *Mechanical properties of 3D-printed materials PLA and PETG used in simulations.*

Material	Young's modulus E (MPa)	Poisson's ratio ν	Density ρ (kg/m³)
PLA	3700	0.35	1200
PETG	2150	0.35	1200

These parameters were later assigned in both FEBio and PrePoMax numerical models to ensure consistency between simulations and experimental testing.

2.2 Experimental setup

The experimental tests were carried out in the vibration laboratory using an electrodynamic shaker (Tiravib 50303) capable of generating sinusoidal excitations over a frequency range of 0–2000 Hz, with a maximum force output of 2 kN. The control loop was managed through a Vibration Research 8500 controller and a Bruel & Kjær 4514-B accelerometer mounted on the shaker armature. Each orthosis was mounted vertically on the shaker platform, being mechanically fastened through a central screw inserted in the sole region to ensure stable and repeatable boundary conditions.

A lightweight DYTRAN 3224A1 piezoelectric accelerometer (mass 0.5 g) was used to record the vibration response, minimizing any influence on the modal behavior of the orthosis. The measurements were performed in two main stages:

• **Impact excitation** (Fig. 2): The orthosis was fixed on the shaker base, which remained inactive during the impact tests. The same mounting configuration was later used for the harmonic excitation stage, ensuring identical boundary conditions across both experimental setups. The vibration response was recorded using a lightweight DYTRAN 3224A1 piezoelectric accelerometer (mass 0.5 g) and a PCB 086D05 impact hammer, both connected to a DEWESOFT SIRIUS data acquisition system operating at a 20 kS/s sampling rate.

The accelerometer was first positioned at the base of the orthosis, and the structure was excited by four hammer impacts applied at different surface points. The sensor was then repositioned to an upper location, and the same impact sequence was repeated. These tests were conducted for both PLA and PETG samples under identical boundary conditions.

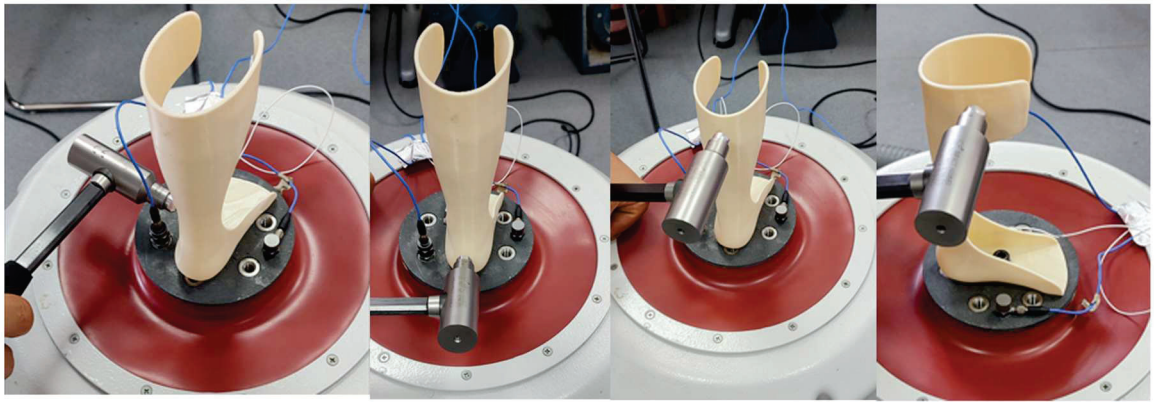

Figure 2. Experimental setup showing hammer impact positions used for free vibration testing of PLA orthoses

• **Harmonic excitation**: the shaker was subsequently activated to perform a low-amplitude (0.5 g peak) sinusoidal frequency sweep within the 1–2000 Hz range. The lightweight accelerometer was placed at a representative location on the orthosis (Fig. 3) to capture steady-state vibration amplitudes.

Data acquisition and signal processing were performed using a Dewesoft Sirius i 8-channel module, connected to a Dell Inspiron 27 7730 All-in-One PC. The Dewesoft software controlled the excitation parameters and recorded the acceleration signals.

The acceleration spectra were analyzed to identify resonance frequencies, modal amplitudes, and differences between materials. Each measurement was repeated multiple times across different sessions, to ensure consistency.

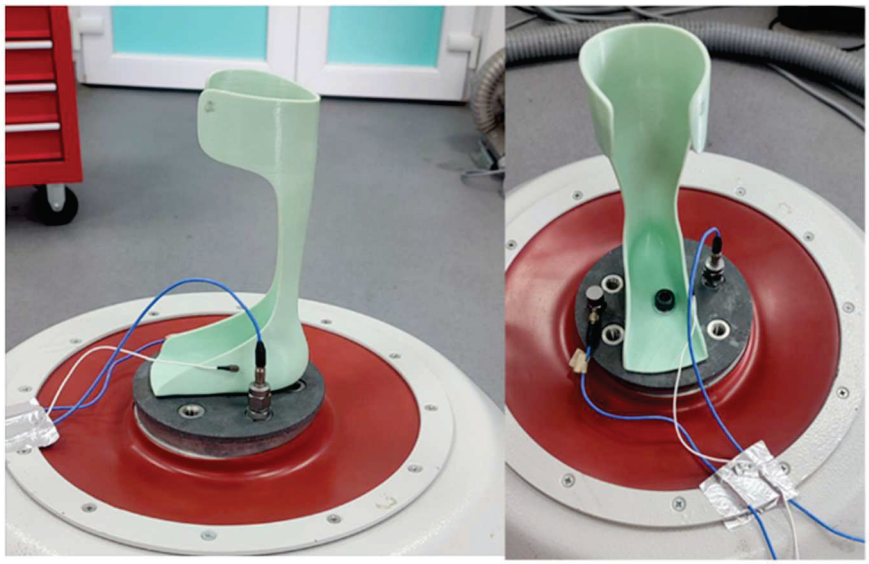

Figure 3. Experimental setup for harmonic excitation (forced vibration) testing of the 3D-printed orthosis mounted on the shaker platform

2.3 Numerical testing

Prior to importing the orthoses into the FEM solvers, a mesh-to-nurbs conversion was completed in Rhinoceros 8, under a trial-period license. The volumetric mesh was then reproduced through the simulation environment algorithms, depending on the specific open-source software used (NetGen in PrePoMax and TetGen in FEBio) – (Fig. 4). Alternatively, the initial mesh could have been imported and remeshed directly, to avoid the use of a license-dependent tool and keep a full open-source approach.

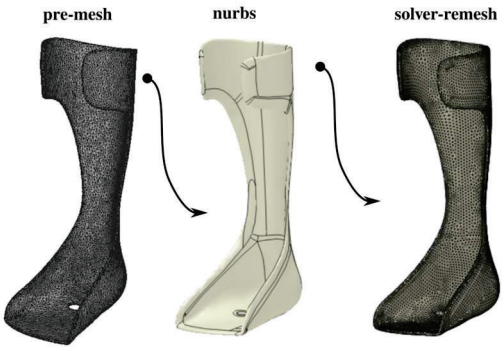

Figure 4. Workflow illustrating the transition from the initial surface mesh to the NURBS model and solver-generated volumetric remesh.

2.4 Natural frequencies in PrePoMax

A modal analysis of the free-response of the system, allowing to directly identify the natural frequencies was performed in PrePoMax, an open-source pre- and post-processor based on the CalculiX solver, which supports both static and dynamic simulations.

The STEP-format nurbs geometry of the ankle–foot orthosis was imported directly from the CAD model and discretized using tetrahedral elements with an element size between 1.0mm and 2.0 mm, consistent with the FEBio mesh parameters. A brief mesh convergence study indicated a frequency deviation between the last (1–2 mm) and the second-to-last (0.5–1 mm) mesh refinements of approximately 0.1–0.4%, depending on the specific natural frequency. This represents an acceptable relative frequency error, $e_f(\%)$, defined as:

$$e_f(\%) = \left|\frac{f_n - f_{n-1}}{f_n}\right| \% = 0.1 - 0.4\% \qquad (5)$$

where n is the last mesh element resizing iteration, $|q|$ is the module operator applied to a scalar quantity "q".

A frequency-domain analysis was conducted to evaluate the forced vibration behavior of the orthosis in the 0–100 Hz range. The lower attachment hole was constrained as to reproduce a similar fixation condition used during experimental testing (Fig. 5).

Figure 5. Fixed boundary condition applied at the lower attachment hole of the ankle–foot orthosis model

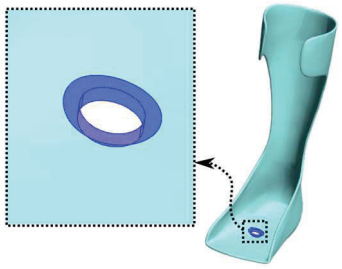

The computed response included displacement amplitudes and mode shapes at the corresponding excitation frequencies. The simulation results were subsequently post-processed to identify resonance peaks and compare modal behavior with both FEBio and experimental data.

2.5 Impulse-based simulation in FEBio

The vibration behavior of the AFOs was numerically investigated using FEBio (Finite Elements for Biomechanics), an open-source finite element software specifically developed for biomechanical systems [6]. The 3D geometry of the orthosis was imported from the CAD model in STL format and discretized using tetrahedral elements, with a minimum element size of 1 mm and a maximum of 2mm.

The same mesh properties and boundary constraints were assigned as in the PrePoMax models to ensure comparable conditions. The material properties were defined according to the values reported in Table 1.

A transient dynamic (impulse-based) analysis was performed by applying a mechanical finite delta-Dirac pulse (triangular signal approximation) to the bottom-lateral surface of the orthosis, corresponding to one of the hammer excitation points used in the experimental setup. The impulse had a peak load of 165 N and a duration of 0.004 s, sufficient to excite multiple natural vibration modes (Fig. 6).

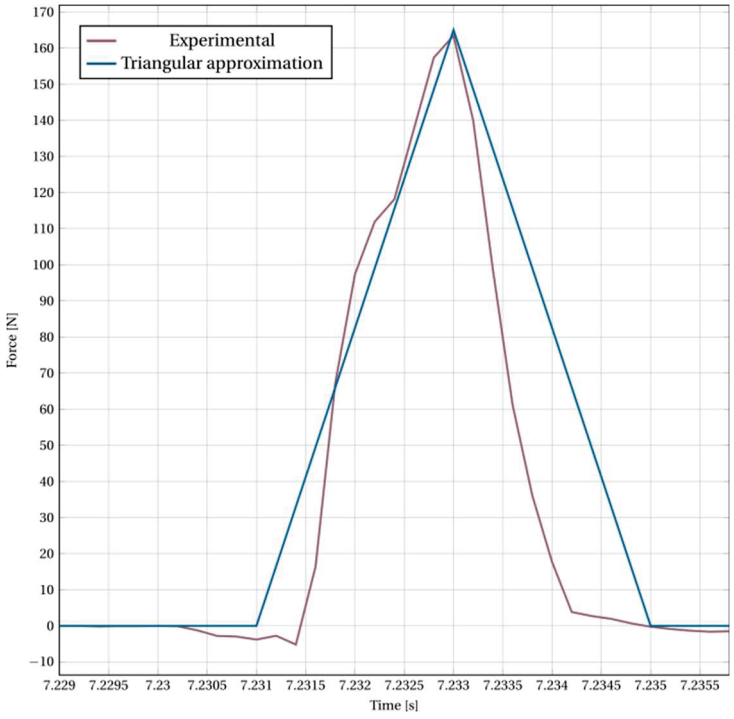

Figure 6. Approximation of the hammer-test experimental impulse with an ideal, triangular signal

The response was evaluated in terms of acceleration components at selected nodes which allowed to clearly identify the resonating frequencies. The simulation results were post-processed to extract vibration response data. A Fast Fourier Transform (FFT) was applied to identify the dominant resonance frequencies of each material.

$$F\{\boldsymbol{M\ddot{u}} + \boldsymbol{Ku}\} = F\{\delta(t)\} \rightarrow [-\omega^2\boldsymbol{M} + \boldsymbol{K}]\boldsymbol{U}(\omega) = \boldsymbol{\Delta_0}(\omega) \qquad (6)$$

From which, $U(\omega)$ can be solved, and then the acceleration:

$$\boldsymbol{A}(\omega) = -\omega^2\boldsymbol{U}(\omega) \qquad (7)$$

In this formulation F denotes the **Fast Fourier Transform (FFT)** operator and the above equation was written for an undamped condition ($\boldsymbol{C} = \boldsymbol{0}$), while $\boldsymbol{\Delta}_0(\omega)$, with its module proportional to a sinc-squared function $|\boldsymbol{\Delta}_0(\omega)| \propto \text{sinc}^2(\omega T/2)$, is generally a vector with three components of which in this particular simulation there's only a non-zero component: the impulse direction is parallel to one of the three axes in the global reference system. Finally, the spectrum system response in terms of acceleration amplitudes can be represented ($\omega = 2\pi f$).

2.6 Data processing

The vibration responses obtained from both experimental and numerical forced-response tests were analyzed in the frequency domain using the Fast Fourier Transform (FFT).
For the impulse-based analyses (experimental impact tests and the FEBio simulation), FFT was directly applied to the recorded acceleration time-series to identify the dominant resonance peaks corresponding to the natural vibration modes.

In the harmonic analysis performed with PrePoMax, the frequency response was obtained directly from the solver output, which provided steady-state modal shapes in terms of displacement amplitude over the 0–100 Hz frequency range.

In all cases, the identified natural frequencies, mode shapes, and relative amplitude ratios were compared across the three approaches (experimental, FEBio, and PrePoMax) to assess their consistency.

Minor variations between results were expected due to differences in damping characteristics, excitation type, and numerical discretization.

3. RESULTS

3.1 Physical testing results

Experimental vibration tests were conducted using both impact excitation and harmonic excitation methods to characterize the dynamic response of the 3D-printed orthoses.
Although measurements covered a wide frequency range (0–2000 Hz), the analysis focused on the same 0–100 Hz spectral window, which includes the most relevant resonance modes for lower-limb orthotic applications and corresponds to the frequency range used in numerical simulations. Examples of recorded responses are shown in Fig. 7.

Each combination of load (impact or shaker) and sensor setup produced a maximum amplitude peak at a specific frequency, corresponding to a resonant mode with a non-zero component in the point and direction detected by the sensor. In each test, one or more resonant frequencies consistently appeared as primary or secondary peaks within the frequency range of interest (0–100 Hz).

Moreover, Tabs. 2 and 3 indicate that, although both the impact and sensor positions were varied, the identified natural frequencies showed similar values, demonstrating the stability of the orthosis' vibration modes.

The FFT analysis of the acceleration signals revealed two distinct resonance regions. The first major resonance occurred at 25–26 Hz for PETG and 34–35 Hz for PLA, consistently observed across multiple sensor positions for both polymeric samples. A second resonance mode was registered near 64–65 Hz for PETG and 85–86 Hz for PLA.

Representative frequency-domain acceleration response plots are shown below.

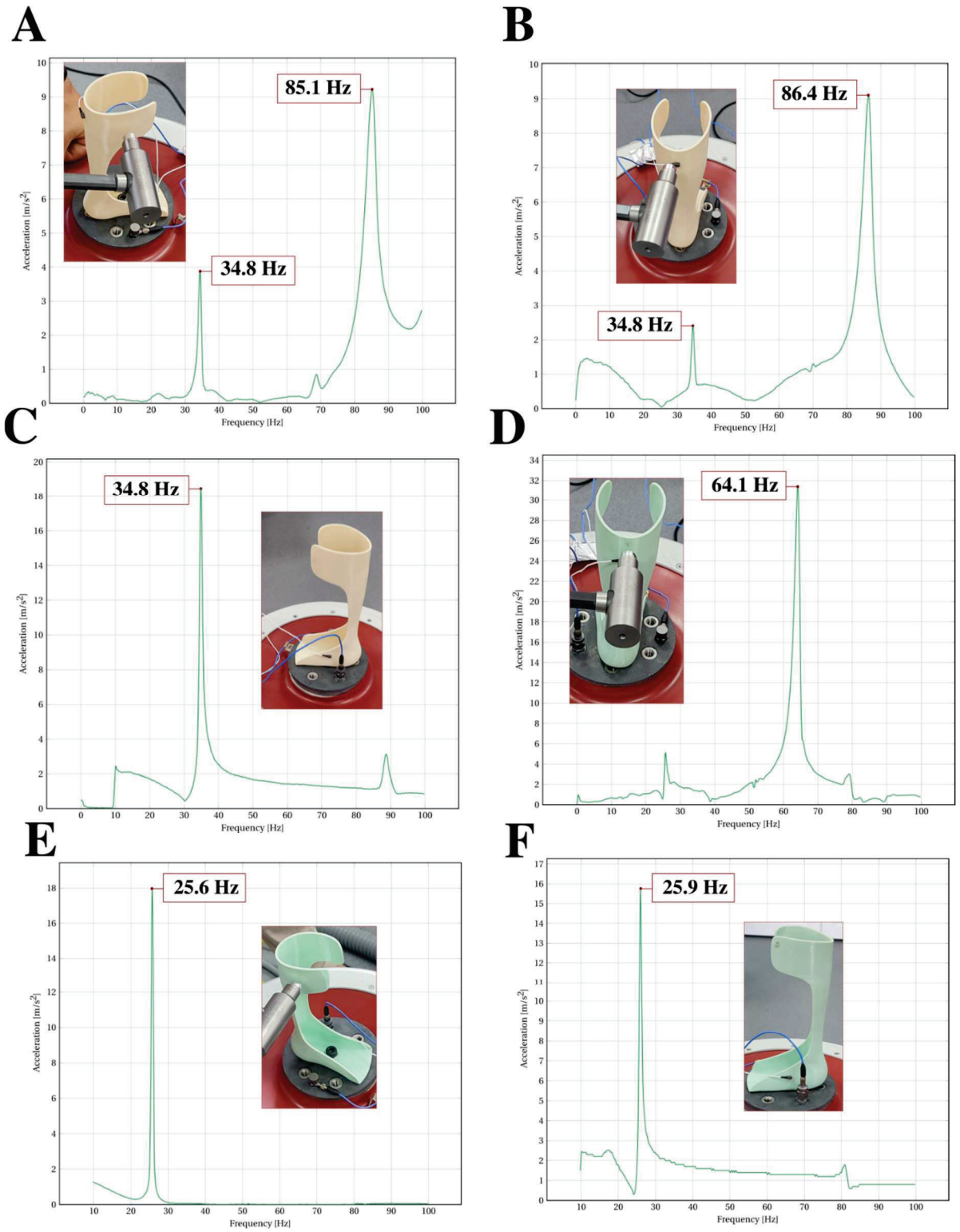

Figure 7. Frequency-domain acceleration spectra for PLA and PETG orthoses under impact and harmonic excitation. When the hammer doesn't appear in the illustrations referring to a specific plot-response, that representation will refer to a shaker test. Figs. 7A to 7C refer to tests on the PLA orthosis, while 7D to 7E on PETG ones.

Table 2.

PETG	Top-posterior acc, max peak f (Hz)	Bottom-lateral acc, max peak f (Hz)
Bottom-posterior impulse	64.4	25.6
Bottom-lateral impulse	64.5	25.6
Top-lateral impulse	25.6	25.6
Top-posterior impulse	64.1	25.6
Shaker	64.7	25.9

Table 3.

PLA (exp, freq Hz)	Top-posterior acc, max peak f (Hz)	Bottom-lateral acc, max peak f (Hz)
Bottom-posterior impulse	86.4	34.8
Bottom-lateral impulse	85.1	34.5
Top-lateral impulse	34.5	34.5
Top-posterior impulse	86.4	34.5
Shaker	86,7	34.8

3.2 PrePoMax results

The modal analysis performed in PrePoMax provided the natural frequencies and corresponding vibration modes of the ankle–foot orthosis (AFO) within the frequency range up to 100 Hz.

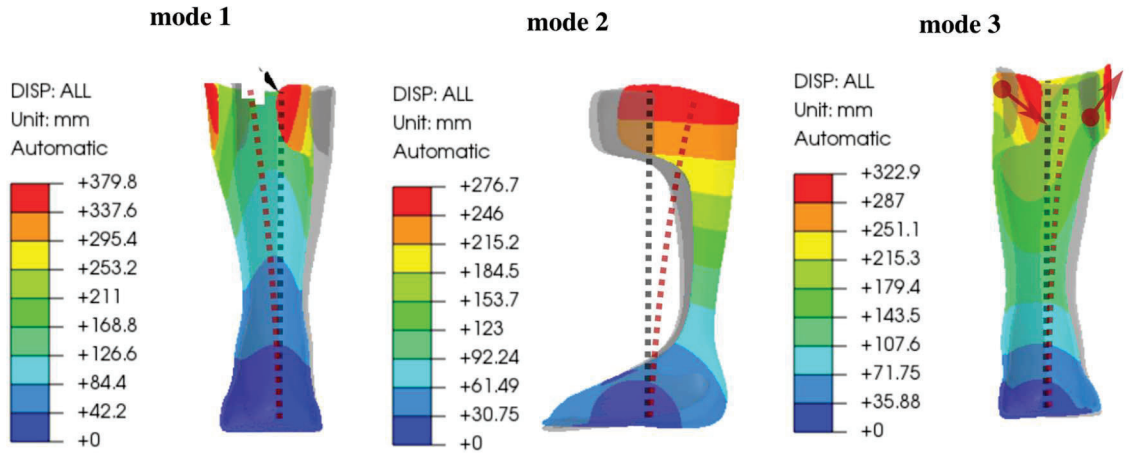

Figure 8. First three modal shapes of the AFO obtained in PrePoMax.

The solver directly computed the natural vibration modes from the stiffness and mass matrices, allowing a clear identification of global and local deformation patterns without time-domain post-processing.

Table 4.

Material	Mode 1 (bending)	Mode 2 (bending)	Mode 3 (bending+torsion)
PETG	24.3 Hz	37.2 Hz	66.2 Hz
PLA	31.8 Hz	48.9 Hz	86.8 Hz

The modal analysis identified three main bending-related modes. The first mode (a) appeared at approximately 24 Hz for PETG and 32 Hz for PLA, the second mode (b) at about 37 Hz for PETG and 49 Hz for PLA, while the third mode (c), characterized by combined bending and torsional deformation, occurred near 66 Hz for PETG and 86–88 Hz for PLA. The first and third modes showed very good agreement with the experimental resonance peaks, confirming the accuracy of the numerical model.

3.3 FEBio results

The impulse-based simulations performed in FEBio provided the transient vibration response of the orthoses following a short lateral mechanical pulse.

The time-domain acceleration data recorded at selected nodes were processed using Fast Fourier Transform (FFT) to identify the dominant frequencies corresponding to the natural vibration modes (Fig 9).

The PLA response exhibited a local vibration mode around 44 Hz, with amplitude increasing progressively toward the lateral wing margin of the orthosis. Both polymers also presented other local modes in specific regions, which were not further analyzed, as this was beyond the primary objectives of the present study.

The main resonance peaks were identified at approximately 27 Hz (mode a) for PETG and 35 Hz for PLA, followed by mode b around 38 Hz (PETG) and 49 Hz (PLA), and mode c near 64 Hz (PETG) and 84–85 Hz (PLA).

Modes a and c were in close agreement with both the experimental findings and the results obtained from the PrePoMax modal analysis, confirming the reliability and consistency of the numerical approach.

Table 5.

Material	Mode a	Mode b	Mode c
PETG	27.1 Hz	38.3 Hz	63.8 Hz
PLA	35.1 Hz	49.4 Hz	84.5 Hz

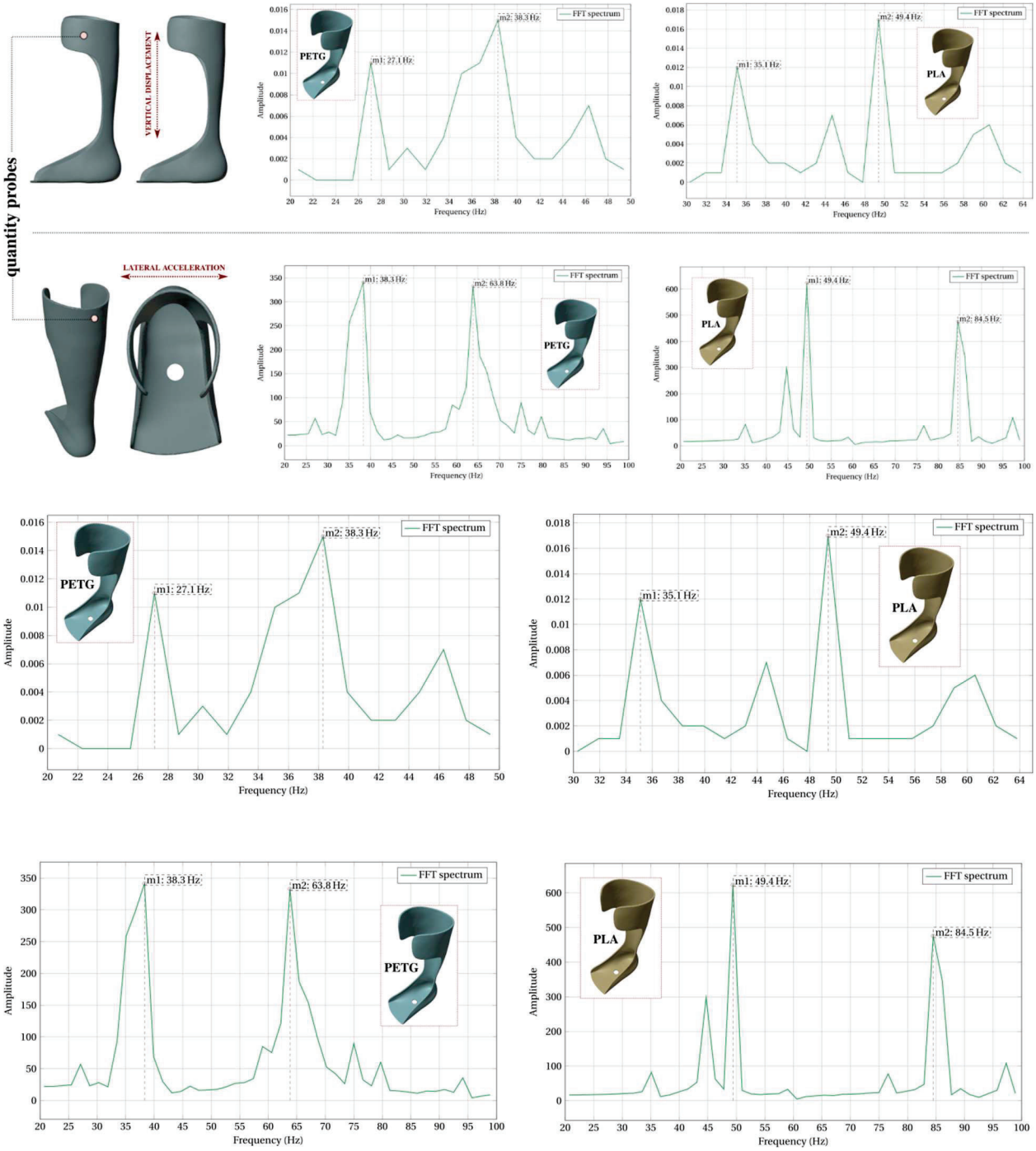

Figure 9. Frequency-domain response obtained from impulse-based FEBio simulations for PETG and PLA orthoses. Using a top-lateral probe, the vertical displacement was measured, while a top-posterior probe was used to analyze the lateral acceleration. The extracted time-dependent amplitude data were then transformed into the frequency domain using FFT.

3.4 Comparison and discussion

Comparative analysis indicated that the natural frequencies predicted by PrePoMax were within 5–10% of those obtained from the FEBio transient simulations and the experimental impact tests (Fig. 10). This degree of accuracy validates both the meshing strategy and the material property definitions used across the models. Minor deviations were mainly attributed to the simplified boundary constraints and the absence of explicit damping control (e.g., Rayleigh α–β parameters) in the purely modal extraction process.

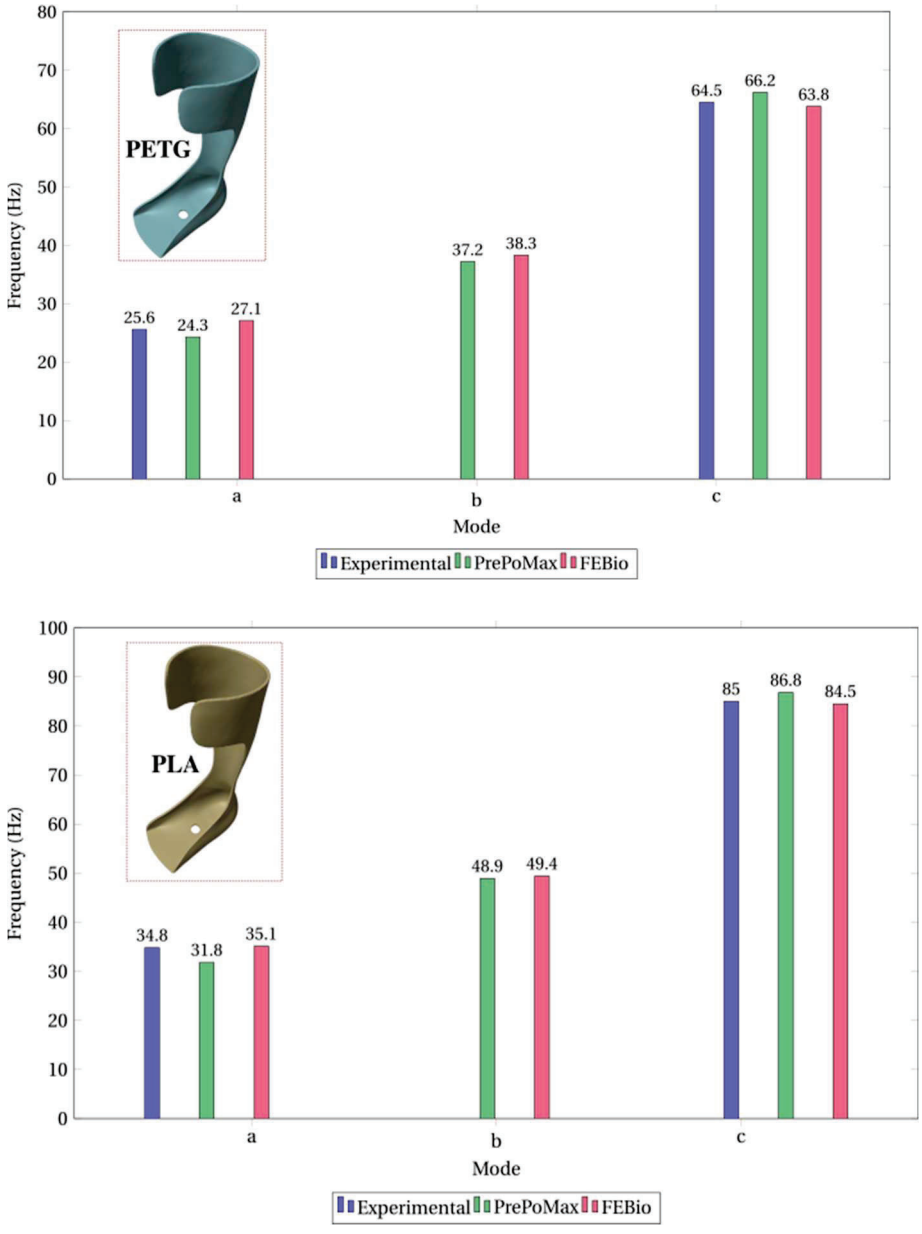

Figure 10. Comparison between experimentally measured and numerically predicted modal frequencies (PrePoMax and FEBio) for PETG (left) and PLA (right) .

The results obtained from experimental testing, FEBio impulse simulations, and PrePoMax modal analyses revealed consistent vibration patterns across all methods. Two main resonance regions were identified, one between 20–40 Hz and another between 60–90 Hz — corresponding to the primary modal shapes of the 3D-printed orthoses. These frequency intervals were consistently observed for both PLA and PETG samples, confirming the reproducibility of their dynamic behavior.

The natural frequencies extracted from simulations were in good agreement with the experimentally measured peaks, indicating that both numerical models successfully captured the structural stiffness and mass distribution of the orthoses. However, amplitude discrepancies were observed, particularly for PLA, which showed slightly higher vibration amplitudes during physical testing compared to numerical results. These differences can be attributed to factors such as microstructural imperfections, interlayer adhesion variability, and residual stresses introduced during FDM printing.

The FEBio simulation slightly overestimates the first mode identified experimentally (whereas PrePoMax slightly underestimates it), while for the second mode, FEBio underestimates and PrePoMax overestimates the experimental result.

Overall, the correspondence between the three approaches validates the experimental setup and confirms that both FEBio and PrePoMax can effectively predict the vibrational characteristics of 3D-printed orthoses within the studied frequency range. The remaining deviations underline the importance of experimental validation and suggest that future work should include nonlinear or viscoelastic modeling to improve the accuracy of numerical predictions.

4. CONCLUSIONS

This study presented an integrated experimental and numerical investigation of the vibration response of 3D-printed ankle–foot orthoses (AFOs) manufactured from PLA and PETG. The experimental tests combined impact excitation and harmonic excitation using an electrodynamic shaker, allowing a detailed characterization of the structural dynamics within the 0 - 100 Hz frequency range.

Complementary finite element analyses were performed using two open-source platforms: PrePoMax, for frequency-domain modal analysis, enabling direct extraction of mode shapes and resonance frequencies;

FEBio, for impulse-based simulations, which captured the natural frequencies and time-domain responses.

Both simulation approaches successfully reproduced the dominant resonance regions identified experimentally, demonstrating good agreement in frequency values and modal behavior. Minor differences in amplitude and damping were observed, mainly due to material anisotropy, interlayer effects, and the simplified linear-elastic models used in the simulations.

The results confirm that open-source tools such as FEBio and PrePoMax can be effectively used to predict and analyze the dynamic response of additively manufactured orthoses. This combined approach reduces reliance on costly commercial solvers and supports the integration of simulation-driven design in orthotic development.

Future research will focus on hyperelastic and viscoelastic material modeling, nonlinear contact conditions, and the inclusion of active vibration control to optimize the performance of next-generation vibration-assisted orthotic devices.

Additionally, further investigations could explore the role of local resonance frequencies through impulse-based simulations and extend the analysis to full-scale or patient-specific AFOs tailored to regulate vibrational behavior.

Acknowledgments: The data presented and analyzed in this study were obtained with the support of INCDT COMOTI's Research and Experiments Center in the field of Acoustics and Vibrations, using their vibration testing and measurement facilities.

Bibliografie

[1] Veltink, P. H., et al. (2009). *Wearable devices for gait analysis*. IEEE Engineering in Medicine and Biology Magazine, 28(2), 38–46.
[2] Telfer, S., & Woodburn, J. (2010). *The use of 3D printing in orthopaedic foot and ankle surgery*. Foot and Ankle Surgery, 16(1), 13–17.
[3] Cardinale, M., & Wakeling, J. (2005). *Whole body vibration exercise: are vibrations good for you?* British Journal of Sports Medicine, 39(9), 585–589, ISSN: 0306-3674, 1473-0480. DOI: 10.1136/bjsm.2005.016857
[4] Cikajlo, I., & Matjacic, Z. (2006). *Directionally specific objective postural response assessment tool: A novel tool for evaluation of postural dysfunction*. Journal of NeuroEngineering and Rehabilitation, 3(1), 6.
[5] Fratini, A., Cesarelli, M., Bifulco, P., & Romano, M. (2009). *Relevance of nonlinearity in surface EMG signal modeling during vibration treatment*. Journal of Biomechanics, 42(10), 1626–1632.
[6] Maas, S. A., Ellis, B. J., Ateshian, G. A., & Weiss, J. A. (2012). *FEBio: Finite Elements for Biomechanics*. Journal of Biomechanical Engineering, 134(1), 011005, ISSN: 0148-0731, 1528-8951. DOI: 10.1115/1.4005694
[7] Antonio Fratini et al. "Relevance of Motion Artifact in Electromyography Recordings during Vibration Treatment". In: Journal of Electromyography and Kinesiology 19.4 (Aug. 2009), pp. 710–718. ISSN:10506411. DOI: 10.1016/j.jelekin.2008.04.005.
[8] Ryo Takeda et al. "Gait Posture Estimation Using Wearable Acceleration and Gyro Sensors". In: Journal of Biomechanics 42.15 (Nov. 2009), pp. 2486–2494. ISSN: 00219290. DOI: 10.1016/j.jbiomech.2009.07.016